13C APSY-NMR for sequential assignment of intrinsically disordered proteins

^{13}C APSY-NMR for sequential assignment of intrinsically disordered proteins

Maria Grazia Murrali[1], Marco Schiavina[1], Valerio Sainati[1], Wolfgang Bermel[2], Roberta Pierattelli[1,3]✉ and Isabella C. Felli[1,3]✉

[1] CERM, University of Florence, Via Luigi Sacconi 6, 50019 Sesto Fiorentino, Florence, Italy

[2] Bruker BioSpin GmbH, Silberstreifen, 76287 Rheinstetten, Germany

[3] Department of Chemistry ‘‘Ugo Schiff’’, University of Florence, 50019 Sesto Fiorentino, Italy

Corresponding Authors

E-mail: felli@cerm.unifi.it; pierattelli@cerm.unifi.it

Abstract

The increasingly recognized biological relevance of intrinsically disordered proteins requires a continuous expansion of the tools for their characterization via NMR spectroscopy, the only technique so far able to provide atomic-resolution information on these highly mobile macromolecules. Here we present the implementation of projection spectroscopy in ^{13}C-direct detected NMR experiments to achieve the sequence specific assignment of IDPs. The approach was used to obtain the complete backbone assignment at high temperature of α-synuclein, a paradigmatic intrinsically disordered protein.

Keywords

Intrinsically disordered proteins, IDPs, assignment, NUS, ^{13}C detection

Introduction

The functional importance of intrinsically disordered proteins (IDPs) or protein regions (IDPRs) has now been widely recognized (Habchi et al., 2014; Wright & Dyson, 2015; van der Lee et al., 2014). Furthermore, a number of key proteins related to the onset of diseases is intrinsically disordered or has large disordered regions (Uversky et al., 2008). Perhaps the most well-known examples include proteins involved in the development of neurodegenerative diseases, such as α-synuclein and Tau for Parkinson's and Alzheimer's diseases. In addition, a vast range of examples of IDPs/IDPRs related to cancer progression are emerging, beyond the most well-known example of p53. These include c-myc, p21, AR, BRCA to name just a few recent examples (Uversky et al., 2014). Therefore, novel approaches to target IDPs or IDPRs are urgently needed in the field of drug discovery (Tóth et al., 2014; Ambadipudi & Zweckstetter, 2016; Joshi et al., 2016; Heller et al., 2017) and in this frame it becomes very important to develop NMR methods to study IDPs/IDPRs in their native state under physiological conditions (Felli and Pierattelli eds., 2015).

The peculiar amino acidic composition of IDPs, often characterized by multiple sequence repetitions and low complexity regions, the high flexibility typical of IDPs/IDPRs and the many conformations sampled in which the protein backbone is largely solvent exposed have an impact on NMR observables that should be considered in the design of effective experimental NMR approaches (Brutscher et al., 2015).

The critical points that need to be faced in order to optimize NMR spectra for the study of highly flexible IDPs/IDPRs include the very low chemical shift dispersion typical of proteins that lack a stable, well defined 3D structure, as well as solvent exchange processes that broaden amide proton resonances when approaching physiological conditions. As known since the early studies on protein folding, heteronuclear spins are characterized by a large chemical shift dispersion and thus well suited to characterize disordered proteins (Dyson & Wright, 2001). Indeed, initial studies of unfolded proteins were stimulated by the development of 3D triple resonance experiments (Kay et al., 1990; Sattler et al., 1999). However, to study unfolded/intrinsically disordered proteins of increasing complexity, a further push in resolution was necessary; a major contribution towards this goal derived from the extension of the dimensionality of NMR experiments to more than three dimensions. Of course methods based on uniform sampling of indirect dimensions and on conventional processing strategies were not suitable to achieve a high resolution in all dimensions, a key aspect to study complex IDPs/IDPRs; different approaches needed to be developed to

render these experiments feasible in a reasonable amount of time and manageable in terms of processing time and disk space. Many non-uniform sampling approaches and different strategies to process the data were indeed proposed (Kupce & Freeman, 2004; Kim & Szyperski, 2003; Hiller et al., 2005; Hoch & Stern, 2001; Orekhov et al., 2003; Kazimierczuk et al., 2006) and initially implemented in triple resonance multidimensional experiments based on H^N detection (Narayanan et al., 2010; Fiorito et al., 2006; Zawadzka-Kazimierczuk et al., 2010; Motackova et al., 2010) and on H^{α} detection (Yao et al., 2014, Mäntylahti et al., 2011) showing a great potential for the characterization of IDPs (Fiorito et al., 2006; Zawadzka-Kazimierczuk et al., 2012; Narayanan et al., 2010; Yao et al., 2014).

In parallel, the increase of the sensitivity of NMR instrumentation (Kovacs et al., 2005) enabled the development of experimental strategies based on heteronuclear direct detection (Bermel et al., 2006c), which turned out to be an excellent tool to study IDPs. Indeed the valuable chemical shift dispersion of heteronuclear spins can be exploited in all dimensions of NMR experiments, including the directly detected one, and limitations deriving from solvent exchange broadening are obviously reduced. Several methods to overcome the problem of ^{13}C homonuclear couplings in the direct acquisition dimension were proposed (Felli & Pierattelli, 2015) and enabled the application of C´ direct detection with high resolution. A suite of 3D multidimensional C´ detected experiments was proposed (Bermel et al., 2009a; Bermel et al., 2009b; Felli et al., 2009; Bermel et al., 2008; Bermel et al., 2006b, O'Hare et al., 2009) and proved to be very useful for sequence specific assignment and characterization of several IDPs. The suite was then expanded to include also C´ detected experiments of dimensionality higher than 3 by implementing random non-uniform sampling in combination with sparse multidimensional Fourier transform (SMFT) processing of the data showing that experiments of higher dimensionality based on C´ detection are indeed possible and constitute a valuable tool to study IDPs (Novácek et al., 2011; Bermel et al., 2012; Novacek et al., 2012; Haba et al., 2013; Bermel et al., 2013; Piai et al., 2014; Baias et al., 2017).

As a further step facilitating the exploitation of the ^{13}C-detection based assignment strategy, we present the implementation of projection spectroscopy for C´ detected multidimensional NMR experiments. The approach is tested on α-synuclein at high temperature.

Material and Methods

Isotopically enriched α-synuclein was prepared as previously described (Huang, Ren et al., 2005) A sample of 1.0 mM uniformly ^{13}C, ^{15}N labeled human α-synuclein in 200 mM NaCl, 0.5 mM EDTA, 20 mM phosphate buffer at pH 6.5 was used. 10 % D_2O was added for the lock.

All the 2D NMR experiments were acquired at 285.5 K, 295 K, 305 K and 315 K while the APSY experiments were all acquired at 315 K on a Bruker AVANCE NEO spectrometer operating at 700.06 MHz ^{1}H, 176.05 MHz ^{13}C and 70.97 MHz ^{15}N frequencies equipped with a cryogenically cooled probehead optimized for ^{13}C-direct detection (TXO). Carrier frequencies and RF pulses suitable for triple resonance ^{13}C detected experiments were used and are summarized hereafter while specific parameters for the different experiments are reported in Table 1. Q5 and Q3 shapes (Emsley & Bodenhausen, 1992) of durations of 300 and 231 μs, respectively, were used for ^{13}C band-selective π/2 and π flip angle pulses, except for the π pulses that should be band-selective on the C^{α} region (Q3, 1200 μs) and for the adiabatic π pulse to invert both C′ and C^{α} (smoothed Chirp 500 μs, 20 % smoothing, 80 kHz sweep width, 11.3 kHz RF field strength) (Böhlen & Bodenhausen, 1993). The ^{13}C band selective pulses on C^{α} and C′ were applied at the center of each region, 53 and 173.5 ppm respectively; the Chirp pulse was centered at 90 ppm. Carrier frequencies for ^{15}N and ^{1}H were 122.5 and 4.7 ppm respectively. Decoupling of ^{1}H and ^{15}N was achieved with Waltz (2.6 kHz) and Garp-4 (1.0 kHz) decoupling sequences respectively (Shaka et al., 1985). All gradients employed had a smoothed square shape. The parameters used for the acquisition of the 5D and 4D experiments as well as the parameters selected to implement the APSY approach are reported in Tables 1 and 2 respectively. FLOPSY-16 (Kadkhodaie et al, 1991) was used in the 4D experiment to spin-lock. All the spectra were acquired using Bruker TopSpin 4.0.1 software. Calibration of the spectra was achieved using DSS as a standard for ^{1}H and ^{13}C; ^{15}N shifts were calibrated indirectly (Markley et al., 1998).

Results and discussion

The 2D ^{1}H-^{15}N HSQC and 2D ^{13}C-^{15}N CON experiments of α-synuclein recorded at various temperatures are reported in Figure 1. It can be noted that the number of cross peaks that can be observed through 2D ^{1}H-^{15}N HSQC spectra decreases with increasing temperature. This is the result of the pronounced exchange processes of amide protons with water protons due to the largely solvent exposed backbone of α-synuclein.

Nuclear spins of non-exchangeable atoms should thus be exploited in NMR experiments. However, even if in principle very sensitive, ^{1}H nuclear spins of aliphatic and aromatic residues are characterized by a quite narrow chemical shift dispersion, in particular when considering amino acids of the same (or similar) type in proteins lacking a 3D structure such as in IDPs. In addition the ^{1}H-^{1}H homonuclear couplings, which are not easy to remove in the direct acquisition dimension, constitute an additional drawback when really high resolution is needed. Instead, non-exchangeable heteronuclear spins, such as ^{13}C and ^{15}N, provide a large chemical shift dispersion even if at the expense of reduced sensitivity when directly detected. Several strategies can be implemented for C´ homonuclear decoupling (Felli and Pierattelli, 2015). Thus, correlations between heteronuclear spins involved in the peptide bond are the most appropriate ones to achieve high resolution (Bermel et al., 2013), as evidenced in the spectra reported in Figure 1 which could be acquired with just a few scans per increment; 2D ^{13}C-^{15}N CON spectra (Bermel et al., 2006a) thus provide a valuable tool to study IDPs at physiological conditions (Gil et al., 2013).

The 2D ^{13}C-^{15}N CON spectra can then be expanded into higher dimensional experiments that provide different types of correlations between different nuclear spins in order to achieve sufficient information for sequence specific assignment. Increasing the number of dimensions however, even when exploiting heteronuclear spins to take advantage of their high dispersion in IDPs, is effective only if we are able to achieve a very high resolution in the indirectly sampled dimensions. This is practically not feasible due to time constraints as well as disk usage unless non-uniform sampling strategies are used, which, combined with appropriate processing strategies, have shown to be very effective (Bermel et al., 2013; Bermel et al., 2012; Novacek et al., 2012; Novacek et al., 2011). Here we test the applicability of projection spectroscopy and of the relative automated data analysis (Hiller et al., 2005) to the C´ detected 5D (HCA)CONCACON experiment (Bermel et al., 2013), which correlates the CON peak of one peptide bond with the preceding one, for the assignment of α-synuclein at high temperature (315 K).

The four orthogonal planes that can be collected through this experiment, reported in Figure 2, show the excellent resolution that can be achieved in all dimensions thanks to the contribution of heteronuclear chemical shifts, in particular of C′ and N that provide correlations across one peptide bond (A) and of C′ and N belonging to the same amino acid (B), as well as sequential C′-C′ correlations (C). The plane correlating C′ and C^{α} (D) is characterized by a somehow reduced resolution but still provides useful information about the amino acid type. These are excellent requisites to implement projection spectroscopy through which not only orthogonal planes but also “transverse” planes cutting the multidimensional object at different angles are acquired with very high resolution as shown in panels E and F of Figure 2. Thanks to the excellent resolution that can be obtained in the projections of C´ detected exclusively heteronuclear experiments, it is possible to resolve the majority of cross peaks in the projections and to identify essentially all correlations expected in the 5D spectrum just by inspection of a limited set of projections. In the present case, 64 projections were acquired with very high resolution (256 points were set in each of the 4 indirect dimensions); it is worth noting that to achieve this kind of resolution for the analogous 5D experiment would have required a prohibitively long time (hundreds of years!). The analysis of the 64 projections, which can be performed automatically by using the algorithm GAPRO (Geometric Analysis of PROjections) (Hiller, Wider et al., 2008; Hiller & Wider, 2012) as it is implemented in the TopSpin 4.0.1 software, provides 191 5D correlations (131 C'_{i-1}, N_i, C^{α}_i, C'_i, N_{i+1} and 60 C'_{i-1}, N_i, C^{α}_{i-1}, C'_{i-1}, N_i). These correlations constitute an excellent tool to achieve sequence specific assignment by linking the shifts of C′ and N involved in a peptide bond with those of the previous one, and also giving some hint on the kind of amino acid through the information of the C^{α} chemical shift. The correlations identified through the GAPRO analysis of the projections are stored in the form of N-dimensional peak-lists that can be manually inspected by loading them on the different projections. In particular, by loading the peak-lists on a 2D ^{13}C-^{15}N CON spectrum the completeness of the assignment can be verified and it is possible to perform the sequence specific walk through the backbone just by moving from one cross peak (C'_i, N_{i+1}) to the neighboring one (C'_{i-1}, N_i), as shown schematically in Figure 3 for a few residues. It is worth noting that for most of these residues the H^N resonance was not observable in ^1H detected experiments.

A few comments are due on technical details related to the implementation of the APSY approach for the 5D (HCA)CONCACON experiment (Bermel et al., 2013). In contrast to the original sequence, the t_2 period was implemented in a semi-constant time manner in order

to increase to possible resolution in this dimension. As noted above, the version presently used yields two types of correlations: type I (C'_{i-1}, N_i, C^{α}_i, C'_i, N_{i+1}) which contains the information for sequential assignment and type II (C'_{i-1}, N_i, C^{α}_{i-1}, C'_{i-1}, N_i) which correlate three nuclear spins (C^{α}_{i-1}, C'_{i-1}, N_i) giving essentially the same information that can be found in 3D CACON experiments. The experiment is optimized to detect correlations of type I; correlations of type II can in principle be suppressed as suggested for the 3D (HCA)CON(CA)H (Mäntylahti et al. 2011). However, in the present case this subset of peaks could be easily identified directly from the peak list and further used for confirming the assignment, so that no further modification of the experiment was required. A few type I correlations were instead missing. Manual inspection of the peak list revealed that most of them involve residues in the known α-synuclein repeats which could not all be safely identified through the automatic algorithm.

A second comment concerns the number of projections that need to be acquired to obtain the information for sequence specific assignment. In the present case we collected projections at 30 different combinations of angles α, β, γ that, considering the issue of quadrature detection in all indirect dimensions, translates into 64 different 2D projections (Table 2). However, processing of the data using a smaller number of projection angles shows that the information content is essentially the same if we use only 26 combinations of angles, as suggested by the software (Hiller & Wider, 2012; Hiller, Wider et al., 2008), and that the number of type I correlations detected in the spectra is only slightly reduced if we consider a smaller subset of angles (Table 3), showing the robustness of this approach. The major issue to be solved was to properly implement in the APSY software the virtual homonuclear decoupling of C´ through the IPAP approach. The processing of the data, including the virtual decoupling, can now be handled very easily through TopSpin 4.0.1.

The APSY approach can of course be implemented in any kind of C´ detected experiment, using the 2D ^{13}C-^{15}N CON spectrum as a reference. For example, the information about the amino acid side chain, can be easily obtained and correlated to each of the cross peaks observed in the 2D ^{13}C-^{15}N CON spectrum, by collecting experiments such as 4D HCBCACON (Bermel et al., 2009) or 4D HCCCON (Bermel et al., 2012). As an example the latter was acquired on α-synuclein and provided information about the vast majority of ^{13}C chemical shifts of aliphatic side chains. Care was taken to implement the ^{13}C evolution in the constant-time mode in order to refocus homonuclear ^{13}C couplings of aliphatic carbons that easily show up in highly resolved projections and can complicate the analysis of

crowded regions. The modified pulse sequence (4D CT-HCCCON) and a few projections to illustrate the quality of the spectra are reported in the Supplementary Material (Figures S1 and S2).

A final comment is due about the amide proton resonances that are still observable approaching physiological conditions. Combination of the C´ detected experiments with H^N detected ones provides a useful tool to achieve unambiguous assignment of the amide proton resonances that are still observable in these conditions. In our case we collected a 3D HNCO experiment, also in the APSY mode, in order to correlate H^N_i resonances with the C'_{i-1}-N_i resonances that we have assigned through C´ detected experiments. Through this approach 93 cross peaks were detected and, thanks to the peak list obtained in a fully automated manner through the GAPRO analysis of the APSY HNCO, the available assignment of heteronuclear spins could easily be extended to the residual H^N resonances that can be detected at this temperature. It is worth noting that a similar result could be achieved by following the temperature dependence of the signals. The latter approach however works well only for well resolved H^N cross peaks but it becomes quite ambiguous for cross peaks in crowded regions of the 2D ^1H-^{15}N HSQC spectra. Therefore the combination of C´ detected experiments with H^N detected ones, even at high temperature and pH, provides unambiguous information to assign H^N resonances that remain also in presence of fast exchange, without ambiguities resulting from temperature dependence of the signals and/or from incomplete information provided by H^N detected spectra. The temperature dependence of H^N, C´ and N spins, once unambiguous assignment is available, might provide also valuable information to investigate variations of exchange processes of amide protons with the solvent upon increasing temperature as well as to highlight possible variations in partially populated local conformations by analyzing heteronuclear chemical shifts. The sequence specific assignment of α-synuclein achieved at 315 K has been deposited in the BMRB (ID 27348).

Concluding, we demonstrate the implementation of the APSY strategy in C´ detected multidimensional NMR experiments. Excellent resolution can be achieved for the 2D cross sections of the high dimensional C´ detected exclusively heteronuclear spectra, showing that the two approaches (APSY and C´ detection) mutually benefit by their joint implementation.

Acknowledgments

The support and the use of resources of the CERM/CIRMMP center of Instruct-ERIC, a Landmark ESFRI project, is gratefully acknowledged. This work has been supported in part by a grant of the Fondazione CR di Firenze and by MEDINTECH (CTN01_001177_962865).

References

Ambadipudi S, Zweckstetter M (2016) Targeting intrinsically disordered proteins in rational drug discovery. Expert Opin Drug Discov 11:65-77

Baias M, Smith PE, Shen K, Joachimiak LA, Zerko S, Koźmiński W, Frydman J, Frydman L (2017) Structure and dynamics of the Huntingtin exon-1 N-terminus: a solution NMR perspective. J Am Chem Soc 139:1168-1176

Bermel W, Bertini I, Csizmok V, Felli IC, Pierattelli R, Tompa P (2009) H-start for exclusively heteronuclear NMR spectroscopy: the case of intrinsically disordered proteins. J Magn Reson 198:275-281

Bermel W, Bertini I, Felli IC, Kümmerle R, Pierattelli R (2006) Novel ^{13}C direct detection experiments, including extension to the third dimension, to perform the complete assignment of proteins. J Magn Reson 178:56-64

Bermel W, Bertini I, Felli IC, Lee Y-M, Luchinat C, Pierattelli R (2006) Protonless NMR experiments for sequence-specific assignment of backbone nuclei in unfolded proteins. J Am Chem Soc 128:3918-3919

Bermel W, Bertini I, Felli IC, Piccioli M, Pierattelli R (2006) ^{13}C-detected protonless NMR spectroscopy of proteins in solution. Progr NMR Spectrosc 48:25-45

Bermel W, Bertini I, Felli IC, Pierattelli R (2009) Speeding up ^{13}C direct detection Biomolecular NMR experiments. J Am Chem Soc 131:15339-15345

Bermel W, Bertini I, Gonnelli L, Felli IC, Koźmiński W, Piai A, Pierattelli R, Stanek J (2012) Speeding up sequence specific assignment of IDPs. J Biomol NMR 53:293-301

Bermel W, Bruix M, Felli IC, Kumar VMV, Pierattelli R, Serrano S (2013) Improving the chemical shift dispersion of multidimensional NMR spectra of intrinsically disordered proteins. J Biomol NMR 55:231-237

Bermel W, Felli IC, Gonnelli L, Koźmiński W, Piai A, Pierattelli R, Zawadzka-Kazimierczuk A (2013) High-dimensionality ^{13}C direct-detected NMR experiments for the automatic assignment of intrinsically disordered proteins. J Biomol NMR 57:353-361

Bermel W, Felli IC, Kümmerle R, Pierattelli R (2008) ^{13}C direct-detection biomolecular NMR. Concepts Magn Reson 32A:183-200

Böhlen J-M, Bodenhausen G (1993) Experimental aspects of chirp NMR spectroscopy. J Magn Reson Ser A 102:293-301

Brutscher B, Felli IC, Gil-Caballero S, Hošek T, Kümmerle R, Piai A, Pierattelli R, Sólyom Z (2015) NMR Methods for the study of instrinsically disordered proteins structure, dynamics, and interactions: General overview and practical guidelines. Adv Exp Med Biol 870:122

Dyson HJ, Wright PE (2001) Nuclear magnetic resonance methods for the elucidation of structure and dynamics in disordered states. Methods In Enzymology 339:258-271

Emsley L, Bodenhausen G (1992) Optimization of shaped selective pulses for NMR using a quaternion description of their overall propagators. J Magn Reson 97:135-148

Felli IC, Pierattelli R (Eds), Intrisically disordered proteins studied by NMR spectroscopy. Springer Switzerland

Felli IC, Pierattelli R (2015) Spin-state-selctive methods in solution- and solid-state biomolecular ^{13}C NMR. Prog NMR Spectrosc 84:1-13

Felli IC, Pierattelli R, Glaser SJ, Luy B (2009) Relaxation-optimised Hartmann-Hahn transfer for carbonyl-carbonyl correlation spectroscopy using a specifically tailored MOCCA-XY16 mixing sequence for protonless ^{13}C direct detection experiments. J Biomol NMR 43:187-196

Fiorito F, Hiller S, Wider G, Wüthrich K (2006) Automated resonance assignment of proteins: 6D APSY-NMR. J Biomol NMR 35:27-37

Gil S, Hošek T, Solyom Z, Kümmerle R, Brutscher B, Pierattelli R, Felli IC (2013) NMR studies of intrinsically disordered proteins near physiological conditions. Angew Chem Int Ed 52:11808-11812

Haba NY, Gross R, Nováček J, Shaked H, Židek L, Barda-Saad M, Chill JH (2013) NMR determines transient structure and dynamics in the disordered C-terminal domain of WASp interacting protein. Biophysical J 105:481-493

Habchi J, Tompa P, Longhi S, Uversky VN (2014) Introducing protein intrinsic disorder. Chem Rev 114:6561-6588

Hiller S, Fiorito F, Wüthrich K, Wider G (2005) Automated projection spectroscopy (APSY). Proc Natl Acad Sci USA 102:10876-10881

Hiller S, Wider G (2012) Automated projection spectroscopy and its applications. Top Curr Chem 316:21-47

Hiller S, Wider G, Wüthrich K (2008) APSY-NMR with proteins: practical aspects and backbone assignment. J Biomol NMR 42:179-195

Hoch JC Stern AS (2001) Nuclear Magnetic Resonance of Biological Macromolecules. pp 159-178

Huang C, Ren G, Zhou H, Wang C (2005) A new method for purification of recombinant human alpha-synuclein in Escherichia coli. Protein Expr Purif 42:173-177

Joshi P, Chia S, Habchi J, Knowles TPJ, Dobson CM, Vendruscolo M (2016) A fragment-based method of creating small-molecule libraries to target the aggregation of intrinsically disordered proteins. ACS Comb Sci 18:144-153

Kadkhodaie M, Rivas O, Tan M, Mohebbi A, Shaka AJ, (1991) Broadband homonuclear cross polarization using flip-flop spectroscopy, J Magn Reson. 91:437–443

Kay LE, Ikura M, Tschudin R, Bax A (1990) Three-dimensional triple-resonance NMR spectroscopy of isotopically enriched proteins. J Magn Reson 89:496-514

Kazimierczuk K, Zawadzka A, Koźmiński W, Zhukov I (2006) Random sampling of evolution time space and Fourier transform processing. J Biomol NMR 36:157-168

Kim S, Szyperski T (2003) GFT NMR, a new approach to rapidly obtain precise high-dimensional NMR spectral information. J Am Chem Soc 125:1385-1393

Kovacs H, Moskau D, Spraul M (2005) Cryogenically cooled probes - a leap in NMR technology. Prog NMR Spectrosc 46:131-155

Kupce E, Freeman R (2004) Projection-reconstruction technique for speeding up multidimensional NMR spectroscopy. J Am Chem Soc 126:6429-6440

Mäntylahti S, Hellman M, Permi P (2011) Extension of the HA-detection based approach: (HCA)CON(CA)H and (HCA)NCO(CA)H experiments for the main-chain assignment of intrinsically disordered proteins. J Biomol NMR 49:99-109

Markley JL, Bax A, Arata Y, Hilbers CW, Kaptein R, Sykes BD, Wright PE, Wüthrich K (1998) Recommendations for the presentation of NMR structures of proteins and nucleic acids. IUPAC-IUPMB-IUPAB inter-union task group on the standardization of data bases of protein and nucleic acid structures determined by NMR spectroscopy. Eur J Biochem 256:1-15

Motackova V, Nováček J, Zawadzka-Kazimierczuk A, Kazimierczuk K, Židek L, Sanderová H, Krásný L, Koźmiński W, Sklenář V (2010) Strategy for complete NMR assignment of disordered proteins with highly repetitive sequences based on resolution-enhanced 5D experiments. J Biomol NMR 48:169-177

Narayanan RL, Duerr HN, Bilbow S, Biernat J, Mendelkow E, Zweckstetter M (2010) Automatic assignment of the intrinsically disordered protein Tau with 441-residues. J Am Chem Soc 132:11906-11907

Nováček J, Haba NY, Chill JH, Žídek L, Sklenář V (2012) 4D Non-uniformly sampled HCBCACON and $^{1}J_{NC\alpha}$-selective HCBCANCO experiments for the sequential assignment and chemical shift analysis of intrinsically disordered proteins. J Biomol NMR 53:139-148

Novácek J, Zawadzka-Kazimierczuk A, Papoušková V, Zídek L, Sanderová H, Krásný L, Koźmiński W, Sklenář V (2011) 5D ^{13}C-detected experiments for backbone assignment of unstructured proteins with a very low signal dispersion. J Biomol NMR 50:1-11

Nováček J, Zawadzka-Kazimierczuk A, Papoušková V, Žídek L, Sanderová H, Krásný L, Koźmiński W, Sklenář V (2011) 5D ^{13}C-detected experiments for backbone assignment of unstructured proteins with a very low signal dispersion. J Biomol NMR 50:1-11

O'Hare B, Benesi AJ, Showalter SA (2009) Incorporating ^{1}H chemical shift determination into ^{13}C-direct detected spectroscopy of intrinsically disordered proteins in solution. J Magn Reson. 200:354-358

Orekhov VY, Ibraghimov I, Billeter M (2003) Optimizing resolution in multidimensional NMR by three-way decomposition. J Biomol NMR 27:165-173

Piai A, Hošek T, Gonnelli L, Zawadzka-Kazimierczuk A, Koźmiński W, Brutscher B, Bermel W, Pierattelli R, Felli IC (2014) "CON-CON" assignment strategy for highly flexible intrinsically disordered proteins. J Biomol NMR 60:209-218

Sattler M, Schleucher J, Griesinger C (1999) Heteronuclear multidimensional NMR experiments for the structure determination of proteins in solution employing pulsed field gradients. Progr NMR Spectrosc 34:93-158

Shaka AJ, Barker PB, Freeman R (1985) Computer-optimized decoupling scheme for wideband applications and low-level operation. J Magn Reson 64:547-552

Tóth G, Gardai SJ, Zago W, Bertoncini CW, Cremades N, Roy SL, Tambe MA, Rochet JC, Galvagnion C, Skibinski G, Finkbeiner S, Bova M, Regnstrom K, Chiou SS, Johnston J, Callaway K, Anderson JP, Jobling MF, Buell AK, Yednock TA, Knowles TP, Vendruscolo M, Christodoulou J, Dobson CM, Schenk D, McConlogue L (2014) Targeting the intrinsically disordered structural ensemble of α-synuclein by small molecules as a potential therapeutic strategy for Parkinson's disease. Plos ONE 9:e87133

Uversky V, Oldfield CJ, Dunker AK (2008) Intrinsically disordered proteins in human diseases: introducing the D2 concept. Annu Rev Biophys 37:215-246

Uversky VN, Davé V, Iakoucheva LM, Malaney P, Metallo SJ, Pathak RR, Joerger AC (2014) Pathological unfoldomics of uncontrolled chaos: intrinsically disordered proteins and human diseases. Chem Rev 114:6844-6879

van der Lee R, Buljan M, Lang B, Weatheritt RJ, Daughdrill GW, Dunker AK, Fuxreiter M, Gough J, Gsponer J, Jones DT, Kim PM, Kriwacki RW, Oldfield CJ, Pappu RV, Tompa P, Uversky VN, Wright PE, Babu MM (2014) Classification of intrinsically disordered regions and proteins. Chem Rev 114:6589-6631

Wright PE, Dyson HJ (2015) Intrinsically disordered proteins in cellular signalling and regulation. Nat Rev Mol Cell Biol 16:18-29

Yao X, Stefan B, Zweckstetter M (2014) A six-dimensional alpha proton detection-based APSY experiment for backbone assignment of intrinsically disordered proteins. J Biomol NMR 60: 231-240

Zawadzka-Kazimierczuk A, Kazimierczuk K, Koźmiński W (2010) A set of 4D NMR experiments of enhanced resolution for easy resonance assignment in proteins. J Magn Reson 202:109-116

1 Zawadzka-Kazimierczuk A, Koźmiński W, Sanderová H, Krásný L (2012) High dimensional and high resolution
2 pulse seqeunces for backbone resonance assignment of intrinsically disordered proteins. J Biomol NMR
3 52:329-337

4

5

6

Figures

Figure 1. ^{1}H-^{15}N HSQC (top) and ^{13}C-^{15}N CON-IPAP spectra (bottom), acquired at different temperatures (285.5 K, 295 K, 305 K, 315 K), showing the temperature dependence for α-synuclein signals. Experiments were acquired at 16.4 T on α-synuclein at pH 6.5.

Figure 2. A subset of the 2D projections acquired with the 5D (HCA)CONCACON experiment are reported to show the quality of the data and to provide an intuitive picture of how the APSY approach works with C´ detected experiments on IDPs (Bermel et al., 2013). Orthogonal projections (A – D) and non-orthogonal ones (E – F) are shown. The spectra were recorded at 16.4 T on α-synuclein at 315 K. The four orthogonal projections correspond to C′(i)-N(i+1), C′(i)-N(i), C′(i)-C′(i±1), and C^{α}(i)-C′(i). In the two non-orthogonal projections the y-coordinate units are arbitrary, as the frequencies in the indirect dimensions are a linear combination of frequencies, that is (E) $\omega_2\sin(45°) + \omega_4\cos(45°)$ and (F) $\omega_1\sin(55°) + \omega_4\cos(55°)$.

Figure 3. As an example the assignment strategy using the peak lists resulting from the GAPRO analysis of the 5D (HCA)CONCACON projections is shown for residues 65-67 of α-synuclein (Bermel et al., 2013). Four five-dimensional “type I” correlations (C'_{i-1}, N_i, C^{α}_i, C'_i, N_{i+1}) are shown. It is worth noting that the amide proton resonances of these residues were not detectable.

Tables

Table 1. Acquisition parameters for 5D ^{APSY}-(HCA)CONCACON (Bermel et al., 2013) and 4D ^{APSY}-HCCCON experiments (Bermel et al., 2012).

Table 2. Values of the projection angles α, β, γ, and of the spectral widths in the dimensions $\omega_{1\text{-}4}$ used here for recording the 2D-projections of the 5D ^{APSY}-(HCA)CONCACON experiment (Bermel et al., 2013). The resulting linear combinations of frequencies are given in the right column.

Table 3. Analysis of the 5D ^{APSY}-(HCA)CONCACON processed considering a reduced number of projection angles as described in the text.

Figure 1

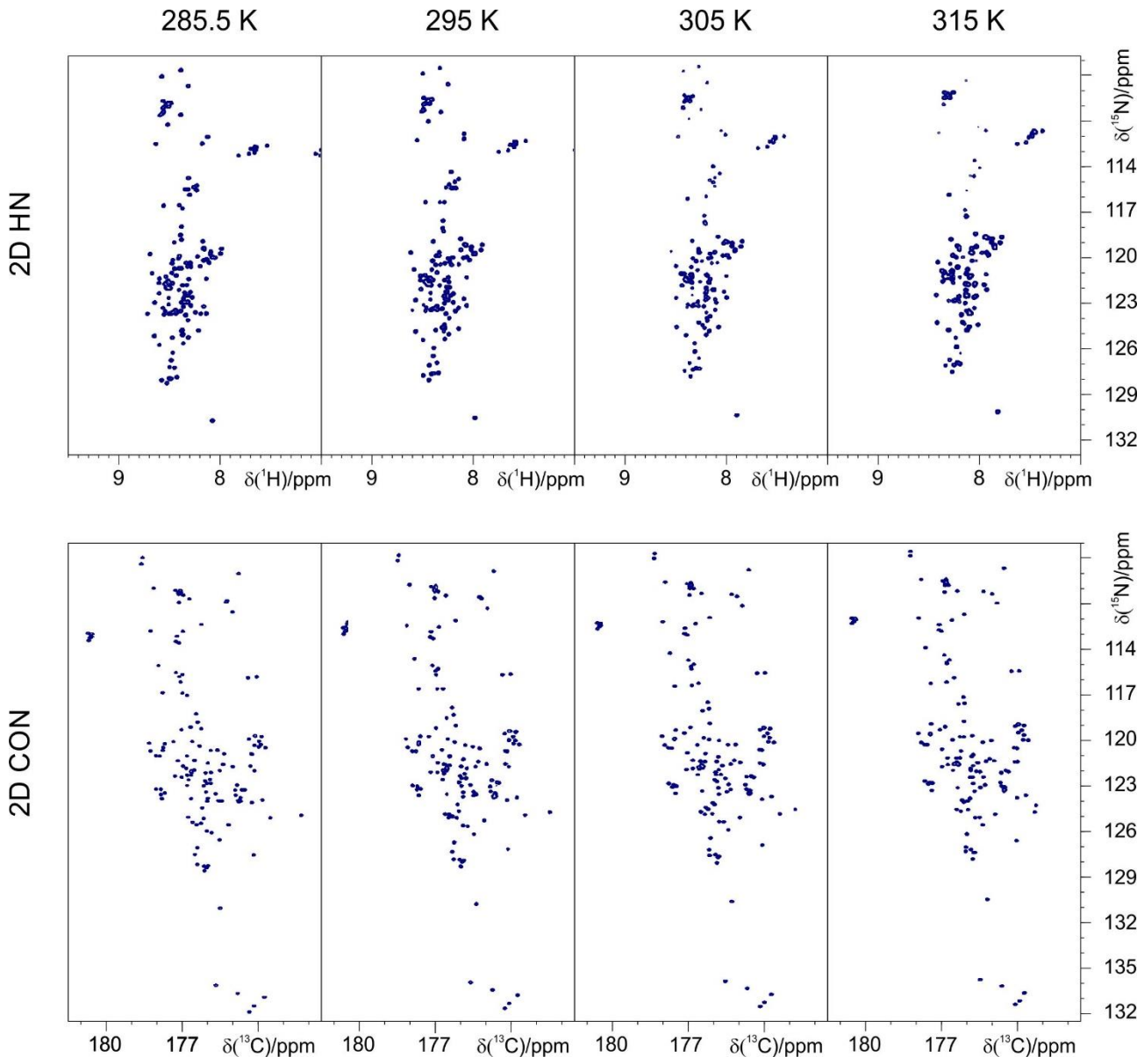
285.5 K
295 K
305 K
315 K
2D HN
2D CON
δ(¹H)/ppm
δ(¹⁵N)/ppm
δ(¹³C)/ppm
9
8
180
177
114
117
120
123
126
129
132
135

Figure 2

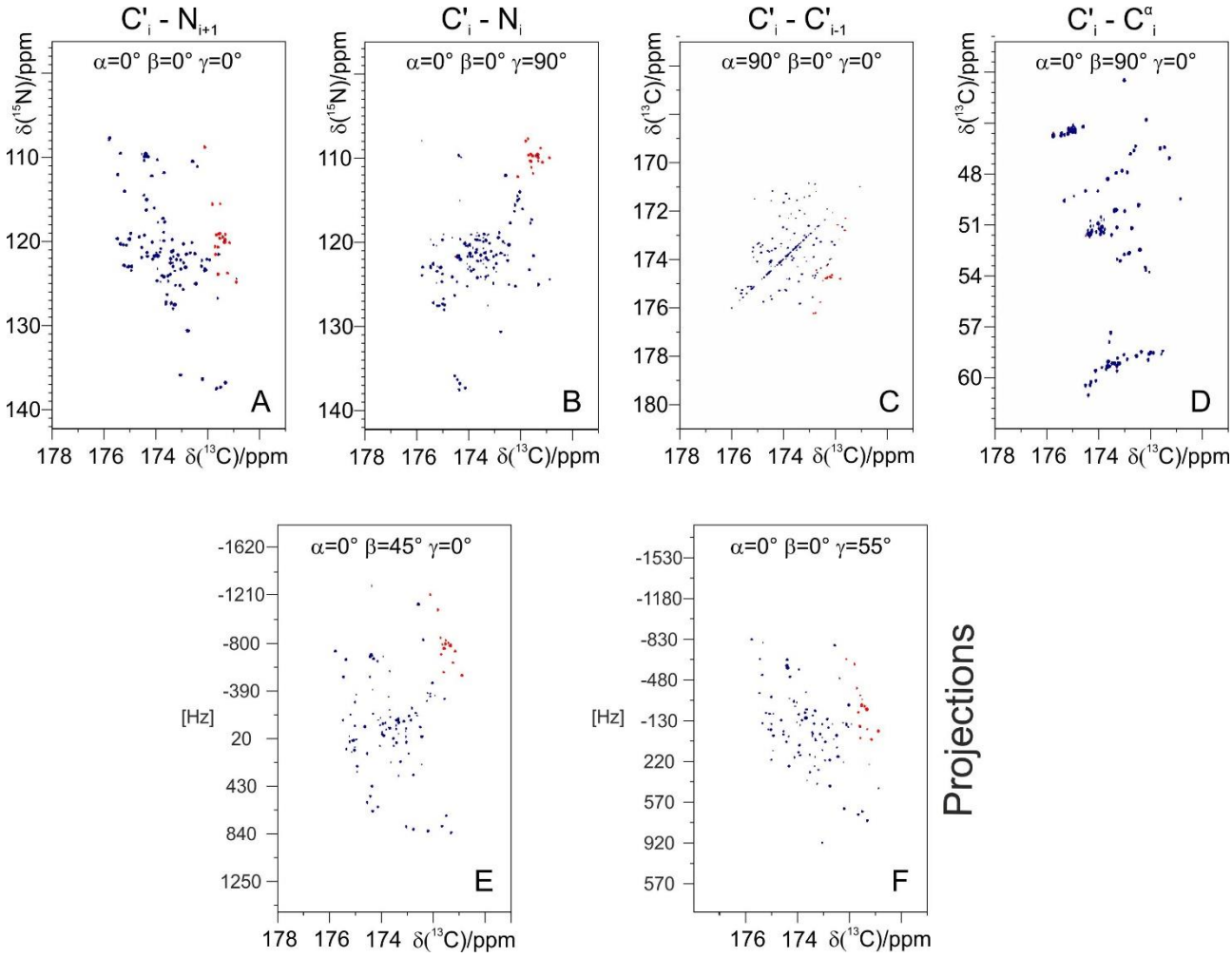
C'i - Ni+1
α=0° β=0° γ=0°
δ(15N)/ppm
A
C'i - Ni
α=0° β=0° γ=90°
B
C'i - C'i-1
α=90° β=0° γ=0°
δ(13C)/ppm
C
C'i - Cαi
α=0° β=90° γ=0°
D
δ(13C)/ppm
α=0° β=45° γ=0°
[Hz]
E
α=0° β=0° γ=55°
F
Projections

Figure 3

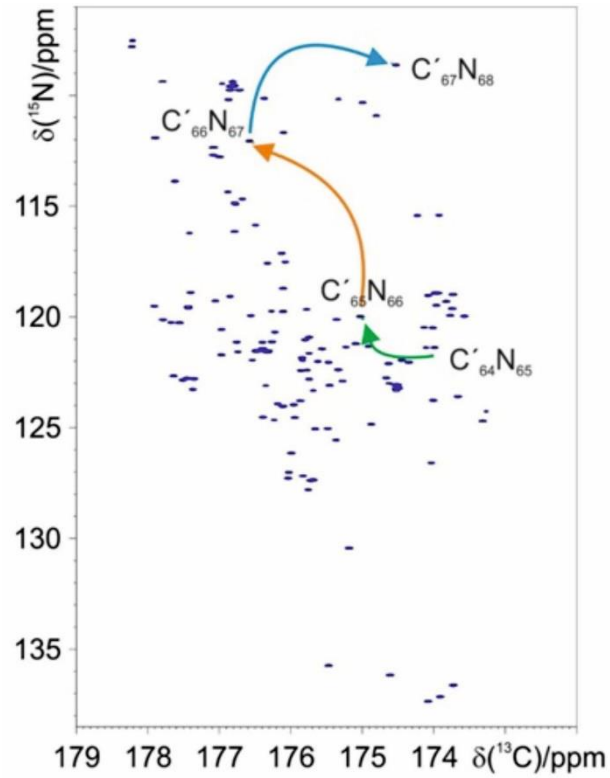

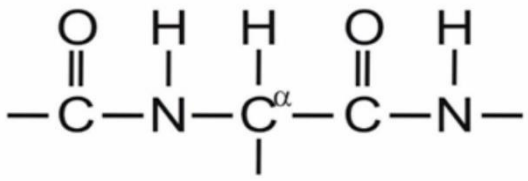

	C'_{i-1}	N_i	C^{α}_i	C'_i	N_{i+1}	
1	176.14	117.14	61.70	173.99	121.42	→ $C'_{64}N_{65}$
2	174.00	121.39	53.16	175.03	120.01	$C'_{64}N_{65}$ → $C'_{65}N_{66}$
3	175.03	119.98	62.53	176.58	112.07	$C'_{65}N_{66}$ → $C'_{66}N_{67}$
4	176.58	112.04	45.39	174.53	108.65	$C'_{66}N_{67}$ →
...	...	...	...	...	...	

Table 1

EXPERIMENT	Spectral width (Hz) & Maximal evolution times				NS	Inter scan delay (s)	Dimension of acquired data					Duration of the experiment	Number of projections
	F1	F2 / F4	F3	F5			F1	F2	F3	F4	F5		
5D (HCA)CONCACON	1695 (^{13}C') 28.4 ms	2404 (^{15}N) 53.2 ms	4505 ($^{13}C^{\alpha}$) 75.5 ms	9090 (^{13}C') 112.6 ms	8	0.8	256	256	256	256	2048	4 days 18 hours	64
	F1	F2	F3	F4									
4D HCCCON	3840 (^{1}H) 66.6 ms	10870 ($^{13}C^{ali}$) 23.6 ms	2404 (^{15}N) 106.5 ms	9090 (^{13}C') 112.6 ms	4	0.8	512	512	512	2048	/	2 days 23 hours	41

Table 2

α	β	γ	Spectral width (Hz)	Linear combination
0°	0°	0°	2404	ω_4
0°	0°	90°	1695	ω_1
0°	90°	0°	2404	ω_2
90°	0°	0°	4505	ω_3
±28°	0°	0°	4238	$\omega_4\cos(28°) \pm \omega_3\sin(28°)$
0°	±45°	0°	3400	$\omega_4\cos(45°) \pm \omega_2\sin(45°)$
0°	0°	±55°	2767	$\omega_4\cos(55°) \pm \omega_1\sin(55°)$
90°	±62°	0°	4238	$\omega_3\cos(62°) \pm \omega_2\sin(62°)$
90°	0°	±69°	3197	$\omega_3\cos(69°) \pm \omega_1\sin(69°)$
0°	90°	±55°	2767	$\omega_2\cos(55°) \pm \omega_1\sin(55°)$
±28°	±41°	0	4775	$\omega_4\cos(28°)\cos(41°) \pm \omega_2\sin(41°) \pm \omega_3\sin(28°)\cos(41°)$
±28°	0°	±51°	3984	$\omega_4\cos(28°)\cos(51°) \pm \omega_1\sin(51°) \pm \omega_3\sin(28°)\cos(51°)$
0°	±45°	±45°	3603	$\omega_4\cos(45°)\cos(45°) \pm \omega_1\sin(45°) \pm \omega_2\sin(45°)\cos(45°)$
90°	±62°	±51°	3984	$\omega_3\cos(62°)\cos(51°) \pm \omega_1\sin(51°) \pm \omega_2\sin(62°)\cos(51°)$
±15°	0°	0°	3488	$\omega_4\cos(15°) \pm \omega_3\sin(15°)$
0°	±27°	0°	3233	$\omega_4\cos(27°) \pm \omega_2\sin(27°)$
0°	0°	±35°	2941	$\omega_4\cos(35°) \pm \omega_1\sin(35°)$
90°	±43°	0°	4934	$\omega_3\cos(43°) \pm \omega_2\cos(43°)$
90°	0°	±53°	4065	$\omega_3\cos(53°) \pm \omega_1\sin(53°)$
0°	90°	±35°	2941	$\omega_2\cos(35°) \pm \omega_1\sin(35°)$
±47°	0°	0°	4934	$\omega_4\cos(47°) \pm \omega_3\sin(47°)$
0°	±63°	0°	3233	$\omega_4\cos(63°) \pm \omega_2\sin(63°)$
0°	0°	±71°	2385	$\omega_4\cos(71°) \pm \omega_1\sin(71°)$
90°	±75°	0°	3488	$\omega_3\cos(75°) \pm \omega_2\cos(75°)$
90°	0°	±79°	2523	$\omega_3\cos(79°) \pm \omega_1\sin(79°)$
0°	90°	±71°	2385	$\omega_2\cos(71°) \pm \omega_1\sin(71°)$
±15°	0°	0°	3488	$\omega_4\cos(15°) \pm \omega_3\sin(15°)$
0°	±20°	0°	3081	$\omega_4\cos(20°) \pm \omega_2\sin(20°)$
±70°	0°	0°	5056	$\omega_4\cos(70°) \pm \omega_3\sin(70°)$
0°	±70°	0°	3081	$\omega_4\cos(70°) \pm \omega_2\sin(70°)$

Table 3

Angle sets	Projections	Experimental time	Identified correlations (Type I)
30	64	4d, 18h	131
26	56	4d, 5h	131
20	44	3d, 9h	129
10	16	1d, 2h	116

^{13}C APSY-NMR for sequential assignment of intrinsically disordered proteins

Maria Grazia Murrali[1], Marco Schiavina[1], Valerio Sainati[1], Wolfgang Bermel[2], Roberta Pierattelli[1,3]✉ and Isabella C. Felli[1,3]✉

Supporting material

Figure S1. Pulse scheme for the 4D CT-HCCCON. The following phase cycling was employed: ϕ_1 = x, -x ; ϕ_2 = 2(y), 2(-y); ϕ_3 = 4(x), 4(-x) ; ϕ_4 = 16(x), 16 (-x); ϕ_5= 8(x), 8(-x), ϕ_{rec}= x, 2(-x), x, (-x), 2(x), (-x), (-x), 2(x), (-x), x, 2(-x), x The quadrature detection was achieved through the States-TPPI approach by incrementing the phase of the π/2 pulse prior to the evolution period; C´ homonuclear decoupling was achieved using IPAP scheme. The length of the delays were: δ= 0.475 ms, Δ= 56 ms, Δ_1= 9 ms , Δ_2= 25ms – p_{12} , ε= $t_3(0)$ + p_8. t_a, t_b and t_c were used to achieve the semi-constant time mode for the ^{1}H indirect dimension. The ^{1}H carrier was placed in the middle of the ^{1}H aliphatic region (2.5 ppm) during the evolution block while it was set at 4.7 ppm in the remaining parts of the pulse sequence.

Figure S2. Examples of 2D projections acquired with the 4D CT-HCCCON experiment to show the quality of the data. Three orthogonal projections (A – C) and a non-orthogonal one (D) are shown. The spectra were recorded at 700 MHz on α-synuclein at 315 K. The three orthogonal projections correspond to C′(i)-N(i+1), C′(i)-Hali(i), C′(i)-Cali(i). The non-orthogonal projection has, as indirect dimension, the combination of $\omega_1$sin(-32°) + $\omega_3$cos(-32°).

Figure S1.

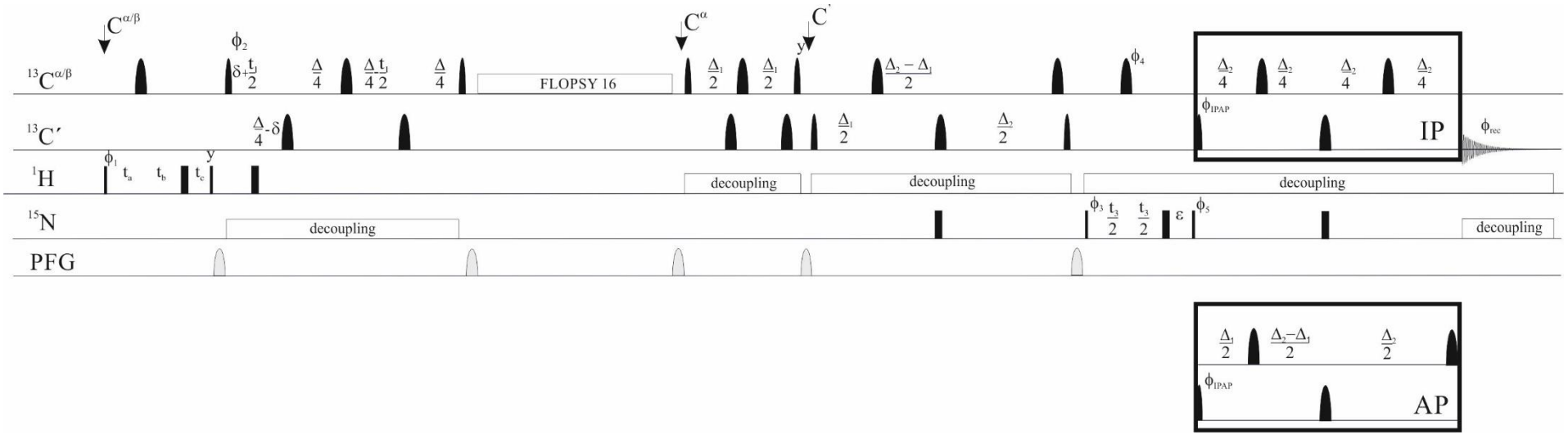
$^{13}C^{\alpha/\beta}$
$^{13}C'$
^{1}H
^{15}N
PFG
FLOPSY 16
decoupling
decoupling
decoupling
decoupling
decoupling
IP
AP

Figure S2

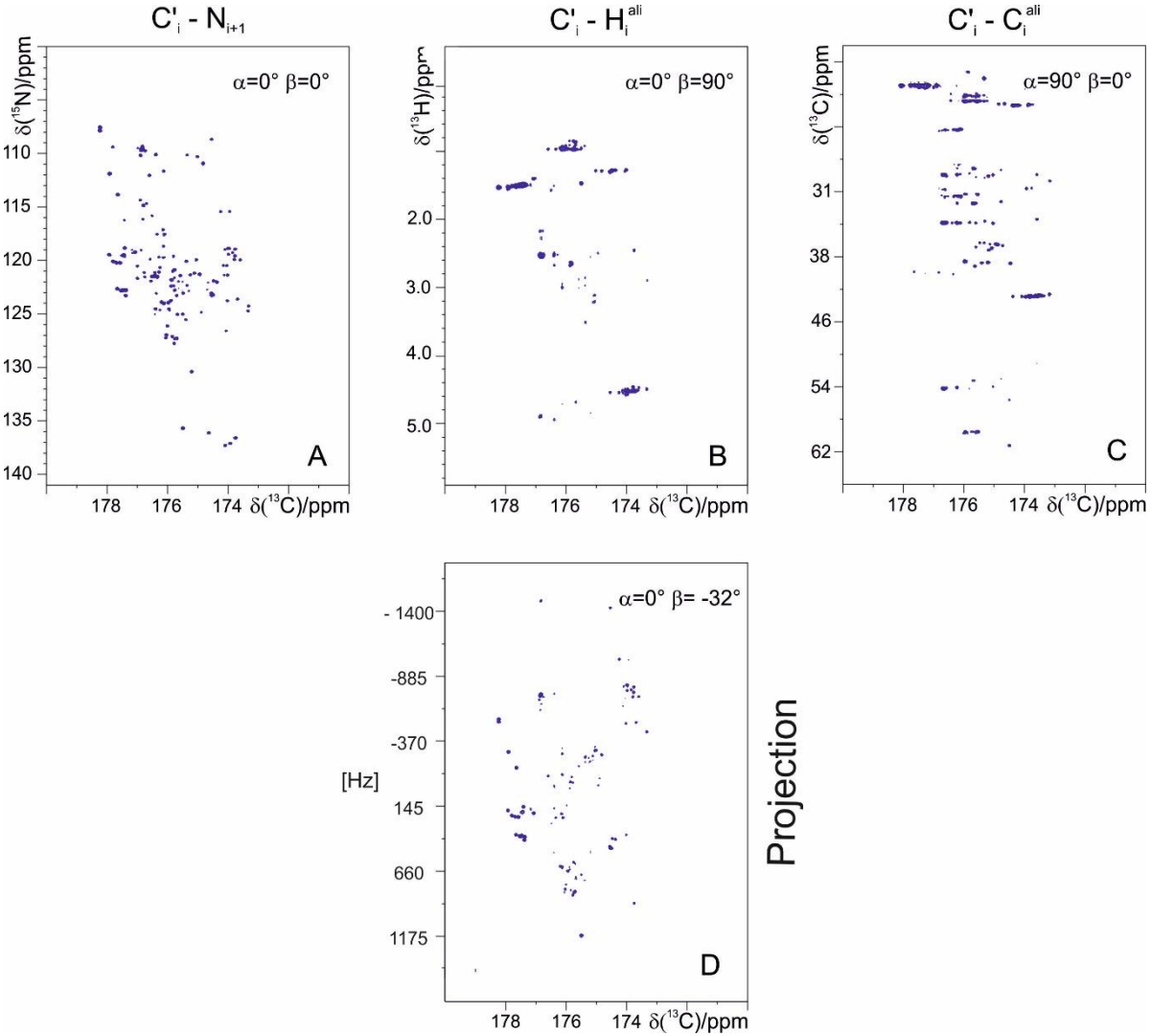
C'i - Ni+1
α=0° β=0°
δ(15N)/ppm
110
115
120
125
130
135
140
178
176
174
δ(13C)/ppm
A
C'i - Hiali
α=0° β=90°
δ(13H)/ppm
2.0
3.0
4.0
5.0
178
176
174
δ(13C)/ppm
B
C'i - Ciali
α=90° β=0°
δ(13C)/ppm
31
38
46
54
62
178
176
174
δ(13C)/ppm
C
α=0° β= -32°
- 1400
-885
-370
[Hz]
145
660
1175
178
176
174
δ(13C)/ppm
D
Projection